STRUCTURE CHARACTERISTICS AND CATALYTIC ACTIVITY OF NICKEL SUPPORTED ON MESOSTRUCTURED CELLULAR FOAM (MCF) SILICA FOR DECARBOXYLATION OF PALMITIC ACID: EFFECT OF TEOS

Lilis Hermida[1,2], Ahmad Zuhairi Abdullah[1]* and Abdul Rahman Mohamed[1]

[1]School of Chemical Engineering, Universiti Sains Malaysia,
14300 Nibong Tebal, Penang, Malaysia.
[2]Department of Chemical Engineering, Universitas Lampung,
Bandar Lampung 35145, Lampung, Indonesia.
*Corresponding author email: chzuhairi@eng.usm.my

ABSTRACT
Mesostructured cellular foam (MCF) silica materials with different pore topology prepared at various amounts of TEOS (9.2; 25; 32 ml) were used as supports for incorporation of nickel. Nickel incorporated MCF catalysts were prepared using deposition-precipitation at 90 ^{o}C and followed by reduction process at 550 ^{o}C. The influence of different pore topology of MCF on characteristics of the nickel incorporated MCF catalysts was studied using nitrogen physisorption, TEM, and SEM-EDX techniques. Activities of the catalysts were tested for decarboxylation of palmitic acid in solvent free condition at reaction temperature of 300 ^{o}C under nitrogen flow for production of n-pentadecane hydrocarbon fuel. The results show that NiMCF-9.2T(R) catalyst using MCF-9.2T support prepared at TEOS amount of 9.2 ml achieved the highest palmitic acid conversion and n-pentadecane yield. The highest activity was mainly attributed to the high nickel composition and a fine nickel particle dispersed in the NiMCF-9.2T(R) catalyst.

Keywords: MCF, Nickel incorporation, Decarboxylation, Hydrocarbon fuel, Palmitic acid.

INTRODUCTION

Fossil fuels depletion and degradation of our environment due to energy production from fossil fuels have been the driving forces for many researchers to study on the development of biofuels as alternative energy sources. Besides renewable energy sources, biofuels are environmentally friendly because they produce lower amounts of greenhouse gases and other air pollutants such as SO_2 and CO [1]. FAME biodiesel is a prominent biofuel mainly produced by transesterification of refined, bleached, and deodorized (RBD) palm oil as feedstock in Malaysia. However, RBD palm oil is mainly used for edible application. This technology faces criticism around the world for using the edible oil as fuels. This situation has encouraged many researchers to investigate for more alternative feedstock and technology for biofuel production.

Palm fatty acid distillate (PFAD), by-product produced from the physical refining of crude palm oil (CPO) to RBD palm oil, is abundantly available in vegetable oil producing countries such as Malaysia and Indonesia [2]. PFAD contains more than 90% free fatty acid (as palmitic acid). It was reported that the average of monthly export prices of PFAD was cheaper compared to those of CPO and RBD palm oil [2]. For that reason, PFAD offers considerable potential as an alternative non-edible feedstock for hydrocarbon fuel production which could decrease the dependency on fossil fuels.

Meanwhile, catalytic deoxygenation, the technology widely established in petroleum industries, is a technique recently developed using non-edible oil feed stock to produce biofuel [3]. Deoxygenation involves removal of molecular oxygen through catalytic decarboxylation or decarbonylation without introducing hydrogen gas. Decarboxylation of non-edible oil, such as fatty acids, is technology that removes molecular oxygen to produce alkane hydrocarbon fuels which are fully compatible with conventional diesel fuel by releasing carbon dioxide, as in Eq.(1) [4]. Meanwhile, decarbonilation process removes molecular oxygen by releasing carbon monoxide and water to produce alkene hydrocarbon fuels. Decarboxylation palmitic acid performed out using catalyst of palladium on synthetic mesoporous carbon Sibunit successfully produced n-pentadecane hydrocarbon fuel [4] having cetane number of 96. Meanwhile standard for diesel fuel is a minimum cetane number of 40 [5].

$$\text{R-COOH} \rightarrow \text{R-H} + CO_2(g) \qquad (1)$$

In addition, Ping *et al.* [6] has successfully carried out catalytic decarboxylation of stearic acid over palladium distributed on MCF material. However, palladium is a precious metal which is expensive. In the present study, fatty acid

decarboxylation over catalyst made from MCF incorporated with inexpensive metal of nickel was studied for the first time. The MCF materials prepared with different TEOS amounts were incorporated with nickel using deposition-precipitation method followed by reduction process. The parent MCF materials and nickel functionalized MCF catalysts were characterized using nitrogen physisorption, TEM, and SEM-EDX techniques. Performance of the nickel dispersed MCF catalyst was examined for production of n-pentadecane hydrocarbon fuel [5] through decarboxylation of palmitic acid, as representative PFAD, at 300 ^{o}C in solvent free condition and without the use of hydrogen.

METHOD

Preparation of MCF silica Material

The MCF silica materials with different structures were synthesized according to previously procedure [7] with modifications. In a typical synthesis 4 g of P123 was dissolved in 70 ml of 1.6 M HCl. Then, 6.8 ml of TMB was added, and the resulting solution was heated to 40 ^{o}C with rapid stirring to synthesis of microemulsion (template). After stirring for 2 h, 9.2 ml of TEOS was added to the solution and stirred for 5 min. Then the solution was transferred into a poly-ethylene bottle and kept at 40 ^{o}C in an oven for 20 h for formation of pre-condensed silica foam. After that, the mixture was removed from the oven and $NH_4F.HF$ (92 mg in 10 ml DI water) was subsequently added to the mixture with slow mixing. Then it was aged at 80 ^{o}C in the oven for 2 days. After cooling, the mixture was filtered and then dried at 100 ^{o}C for 12 h. After that, calcination was carried out in static air at 300 ^{o}C for 0.5 h and 500 ^{o}C for 6 h to remove the template to produce MCF-9.2T. Other MCF materials were synthesized using the same procedure as described above, except the amount of TEOS added, i.e. MCF-25T for TEOS amount of 25 ml and MCF-32T for TEOS amount of 32 ml. The calcined MCF silica materials were used as support for incorporation of Ni.

Incorporation of nickel (Ni) on MCF silica materials

MCF-9.2T, MCF-25T and MCF-32T materials were functionalized with nickel using deposition precipitation method adopted from Nares *et al.* [8]. In the functionalization, 250 ml of an aqueous solution containing 10.156 g of $Ni(NO_3)_2.6H_2O$ and 0.3 ml of HNO_3 69% wt/wt was prepared. In a typical preparation, 40 ml of the aqueous solution was used for dissolving 6.3 g urea at room temperature to make an urea solution and 210 ml of the aqueous solution was mixed with 1.9 g of the MCF material to make suspension. The suspension was heated at 40 ^{o}C, then mixed with the urea solution under rapid mixing. After that, the mixture was heated to 90 ^{o}C for 2 h under static condition. After cooling, the mixture was filtered and the solid was washed three times with 20 ml distilled hot water (~50 ^{o}C), then dried at 100 ^{o}C for 12 h. Then, the solid was calcined in static air at 300 ^{o}C for 6 h. The calcined catalysts were designated as NiMCF-9.2T(C), NiMCF-25T(C) and NiMCF-32T(C). Then the samples were reduced at 550 ^{o}C for 2.5 h under hydrogen stream, and then cooled to room temperature with nitrogen flow. The reduced catalysts were designated as NiMCF-9.2T(R), NiMCF-25T(R) and NiMCF-32T(R).

Characterization

Nitrogen adsorption–desorption isotherms were measured using a Quanta-chrome Autosorb 1C automated gas sorption analyzer at liquid nitrogen temperature. Prior to the experiments, samples were degassed ($P < 10^{-1}$ Pa) at 270 ^{o}C for 6 h.. Specific surface area (S_{BET}) were calculated using BET method, while Barrett-Joyner-Halenda (BJH) model was applied to obtain distribution of cell sizes and window pore sizes using adsorption and desorption isotherms data, respectively.

Samples were also analyzed with SEM/EDX using Leo Supra 50 VP field emission SEM, equipped with an Oxford INCAX act, energy dispersive X-ray microanalysis system. Prior to analysis, samples were mounted on stubs with double-sided adhesive tape. Then, the samples were coated with high purity gold and observed at room temperature.

TEM images were provided by Philips CM 12 transmission electron microscope. Before the TEM analysis, sample of about 0.08 g was first dissolved in a 5 ml of 100 % ethanol. Then, the solution was shaken for a moment; and subsequently a small amount of the solution was taken using a micropipette and dropped on a metal grid for the analysis

Decarboxylation reaction

Decarboxylation of palmitic acid was performed in a semibatch mode in which carbon dioxide produced during the reaction was continuously removed. The decarboxylation was carried out in a 250 mL three-necked flask reactor equipped with a magnetic stirring bar, reflux condenser and a tube to pass pure nitrogen flow to reaction mixture. During decarboxylation reaction, the nitrogen stream swept evolved carbon dioxide through condenser and a carbon dioxide trap

containing 50 ml of 1 M sodium hydroxide, as shown in Figure 1. The reactor was placed on a hot plate. Palmitic acid (4.5 g) and catalyst (0.45 g) were added to the reactor. Before an experiment was started, nitrogen flow was passed through the reaction mixture for 30 min. Then, the reaction mixture was heated to 300 ^{o}C and maintained for 6 h to perform decarboxylation of palmitic acid without solvent under rapid stirring and nitrogen flow. The liquid product was collected after filtering solid phase catalysts. The liquid products were analyzed by means of a GC system equipped with a flame ionization detector and a non-polar capillary column (GsBP-5).

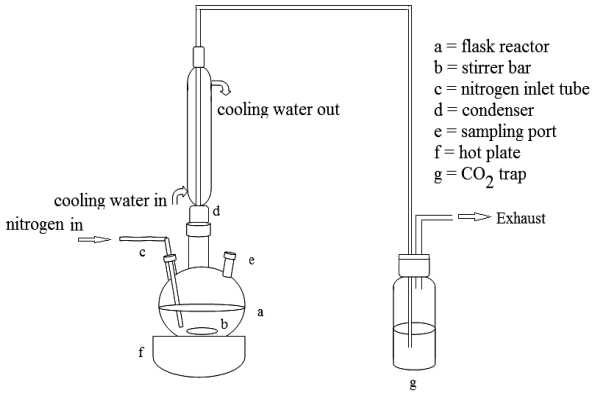

Fig. 1: Catalytic activity test system for decarboxylation of palmitic acid.

RESULTS AND DISCUSSION

Catalyst characterization

Schematic cross section of MCF material as reported in the literature is of strut like structure, as given in Figure 2 (a), showing that the cells of the MCF structure are framed by the silica struts [9]. The characteristic structural feature of MCF material can be confirmed through TEM image of MCF-25T material as shown in Figure 2(b), indicating disordered array of silica struts which are composed of uniform-sized spherical cells interconnected by window pores. This observation proved the successful synthesis of MCF material in this study.

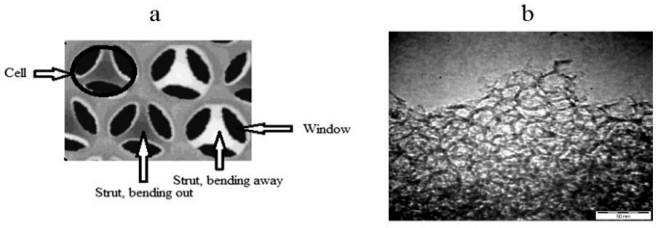

Fig. 2: Feature of MCF silica material, (a): Schematic cross section adopted from Schmidt-Winkel et al. [11], (b): TEM image of MCF-25T.

Table 1 shows textural characteristic of MCF materials prepared at different TEOS amounts and their functionalization with nickel, based on the nitrogen adsorption-desorption data. It can be seen from the table that an increase in TEOS amount from 9.2 ml to 25 ml in preparation of MCF silica materials resulted in the increase in total surface area of the MCF silica material but its pore volume, cell size and window pore size tended to decrease indicating that thicknesses of the MCF walls increased. However, further increase in TEOS amount from 25 ml to 32 ml caused the total surface area and pore volume declining whilst the cell size increased and the window pore size was stable. The main reason of the above phenomenon was attributed to a higher number TMB/P123 microemulsion droplet that interacts with positively protonated silicate species from TEOS to the formation of the 'soft silica" –coated TMB/P123 microemulsion droplets. Then condensation of silica in the walls led to a higher formation of Si-O-Si linkages in the form of mesostructure in the MCF. Meanwhile, the use of an extra TEOS amount in the synthesis interrupted the condensation of the silica network that resulted in a detrimental effect to the formation of mesostructure in the MCF [10].

Table 1: Textural characteristics of MCF materials and those of corresponding nickel functionalized MCF catalysts.

Sample	S_{BET} (m^2/g)	V_{pore}(cm3/g)	d_{cell}(Å)	$d_{window\ pore}$ (Å)
MCF-9.2T	375	2.24	232	130
MCF-25T	404	1.62	231	102
MCF-32T	336	1.41	235	102
NiMCF-9.2T(R)	281	1.02	184	125
NiMCF-25T(R)	324	1.05	230	100
NiMCF-32T(R)	309	0.92	235	100

d_{cell} and $d_{window\ pore}$ are cell size and window pore diameter, repectively, determined withBJH method, S_{BET} is surface area determined based on BET method, and V_{pore} is total pore volume determined at a relative pressure of 0.9948

Moreover, incorporation of nickel particle on MCF silica materials tended to result in a decrease in textural parameters like total surface area, total pore volume, cell size and window pore size. It can be noted from Table 1 that, after incorporation of nickel in MCF-9.2 material, its functionalized product had the highest decrease in total surface area (from 375 to 281 m^2/g), pore volume (from 2.24 to 1.02 cm^3/g), cell size (234 to 184 Å) and window pore size (from 130 to 125 Å). This result indicated the greatest densification of the silica walls with nickel particles inside the NiMCF-9.2T(R) catalyst compared to that occurred inside NiMCF-25T(R) and NiMCF-32T(R) catalysts. The functionalization of MCF-9.2T also resulted in a significant reduction of nitrogen adsorption-desorption isotherms in NiMCF-9.2T(R) as shown in Figure 3. However, the form of nitrogen adsorption-desorption isotherms were not appreciable change after functionalization of all MCF materials prepared. All nitrogen adsorption-desorption isotherms shown in Figure 3 are of type IV because hysteresis in multilayer range of physisorption isotherms occurs, which is often associated with capillary condensation (the pore filling process) in mesopore structure [11]. The nitrogen adsorption-desorption isotherm are in close agreement with those published previously [9] and exhibits a large H1 hysteresis loop,which suggests that the MCF material possesses cell-type mesopores connected by smaller window pores. Type IV adsorption isotherms usually flatten at high P/P0 indicating that the mesopore filling is complete [12]. However, final upward turn was observed for all the isotherms curves shown in Figure 3. This is due to capillary condensation in macropores or in interstices between grains as reported in the literature [13].

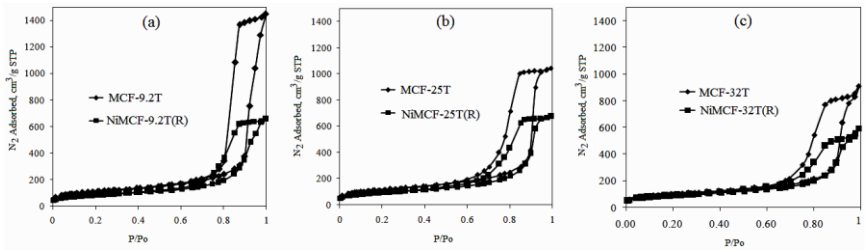

Fig. 3: Nitrogen adsorption-desorption isotherm of MCF silica prepared at different TEOS amounts and their corresponding nickel functionalized MCF catalyst after reduction process

The MCF silica materials with different structural characteristics which were incorporated with nickel were examined using SEM while chemical composition was determined using EDX. The results are shown in Figure 4. As can be seen, the morphology of the nickel functionalized MCF catalysts was strongly influent by the structural characteristics of the MCF supports. For MCF support prepared at TEOS amount of 9.2 ml in the synthesis, uniform nickel nanoparticles in the form of nanoworms were well dispersed in the framework of the MCF-9.2T, as shown in Figure 4(a). The figure also shows that the corresponding nickel functionalized MCF catalyst, i.e. NiMCF-9.2T(R) possessed a high porous structure located between the nanoparticles space. NiMCF-9.2T(R) was found to contain metallic nickel of 5.3 wt. %. With increasing TEOS amount in the synthesis of MCF silica material from 9.2 ml to 25 ml, layered and platelet structures of metallic nickel were observed at NiMCF-25T(R) catalyst, as can be seen in Figure 4(b). Meanwhile, composition of metallic nickel in the NiMCF-25T(R) catalyst was found to be 3.1 wt.% which was lower than that in the NiMCF-9.2T(R). The use of TEOS amount above 25 ml in the synthesis of MCF silica material resulted in abundant layered and platelet structures of metallic nickel with thicker and bigger sizes as can be in NiMCF-32T(R), as shown in Figure 4(c). The NiMCF-32T(R) contained metallic nickel of 14.09

wt. %. It is important to note that although nickel content in NiMCF-9.2T(R) was lower than that in NiMCF-32T(R), the size of metallic nickel particles dispersed in the NiMCF-9.2T(R) was smaller than that in NiMCF-32T(R). Besides that, NiMCF-9.2T(R) possessed a higher porous structure than NiMCF-32T(R). This observation was consistent with result from Table 1 confirming that window pore size of NiMCF-9.2T(R) i.e. 125 Å was larger than that of NiMCF-32T(R), i.e. 100 Å.

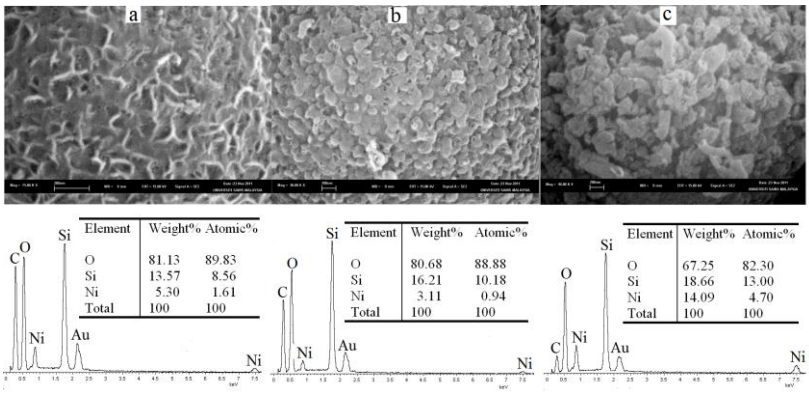

Fig. 4: SEM images (up) together with chemical composition (down) of (a): NiMCF-9,2T(R), (b): NiMCF-25T(R) and (c): NiMCF-32T(R).

Decarboxylation of palmitic acid

Catalytic performances of nickel supported on MCF silica catalysts with different surface characteristics and nickel compositions were evaluated in decarboxylation of palmitic acid at 300 ^{o}C in solvent free condition under nitrogen flow for 6 h. The conversions of palmitic acid and n-pentadecane yields resulting from the experiment run are shown in Table 2. NiMCF-9.2T(R) catalyst exhibited palmitic acid conversion and n-pentadecane yield of 59% and 13 %, respectively, which were the highest conversion and yields compared to those exhibited by NiMCF-25T(R) and NiMCF-32T(R) catalysts. Meanwhile, NiMCF-25T(R) achieved the lowest palmitic acid conversion (3.1 %) and n-pentadecane yield (1.2 %). This result was attributed to a lowest nickel content in the NiMCF-25T(R) catalyst (3.11 wt. %) than that in NiMCF-9.2T(R) catalyst (5.30 wt. %) as confirmed in EDX analysis results. Metallic nickel species were active sites which can produce n-alkane and carbondioxide in decarboxylation of fatty acid through bond cleavage between carboxylic carbon and α carbon as reported in the literature [14]. However, although NiMCF-32T(R) catalysts had the higher nickel composition i.e. 14.09 wt. %, palmitic acid conversion and n-pentadecane yield achieved by the NiMCF-32T(R) were lower than those achieved by NiMCF-9.2T(R). This could be due to a finer nickel particles which were dispersed in NiMCF-9.2T(R) compared to that in NiMCF-32T(R) as confirmed from SEM images in Figure 4. It is reported in the literature that for most metal supported catalysts, the finer active metal particles dispersed in supports may also lead to the higher catalytic activity of the catalysts [15]. In summary, the higher concentration of nickel particles and the finer nickel particle dispersed in the nickel functionalized MCF catalysts contributed to the higher palmitic acid conversion and pentadecane yield in the decarboxylation process.

Table 2: Reaction results of decarboxylation of palmitic acid over 10 wt. % nickel functionalized MCF silica catalysts at 300 ^{o}C in solvent free condition and without hydrogen flow for 6 h.

Catalysts	Palmitic acid conversion, %	n-Pentadecane yield, %
NiMCF-9.2T(R)	59.0	13.0
NiMCF-25T(R)	3.1	1.2
NiMCF-32T(R)	33.4	5.6

Previously, decarboxylation of palmitic acid in dodecane as solvent with a concentration of 0.05 M had been carried out over 4 wt. % palladium supported on synthetic mesoporous carbon Sibunit catalyst at 300 ^{o}C under 5 % H_2 in Argon for 3 h [4]. The catalytic activity results showed that the catalyst achieved a high palmitic acid conversion (98 %) and n-petadecane selectivity (99 %). However, although the catalyst showed a high catalytic activity, the reaction required the use of solvent

and hydrogen. Besides that, palladium is rare and expensive. Meanwhile, Roh *et al.* [14] recently observed decarboxylation of oleic acid in solvent free condition and without the use of H_2 flow over 20 wt. % nickel supported on $MgO\text{-}Al_2O_3$ catalyst. The catalyst achieved oleic acid conversion of 31% with heptadecane selectivity of 3.7 % at the reaction operated at 300 ^oC for 3 h.

CONCLUSION

Preparations of MCF silica supports with different characteristics by varying TEOS amount (9.2ml, 25ml, and 32 ml) were successfully carried out. The increase in TEOS amount resulted in the increase in total surface area but its pore volume, cell size and window pore size were found to decrease due to a higher formation of Si-O-Si linkages . Further increase in TEOS amount caused detrimental effect to the formation of the mesostructure in the MCF as condensations of the silica network were interrupted by the excess TEOS amount. After functionalization of MCF silica materials with nickel, the surface area, total pore volume, cell size and window pore size decreased indicating the successful incorporation of nickel in the MCF materials.

Among the MCF silica materials, MCF prepared using TEOS amount of 9.2 ml (MCF-9.2T) was promising support for incorporation of nickel as the produced catalyst i.e. NiMCF-9.2T(R) achieved the highest palmitic acid conversion and n-pentadecane yield in decarboxylation of palmitic acid at 300 ^oC in solvent free condition and under nitrogen flow. The highest catalytic activity was attributed to the high nickel composition and a fine nickel particle dispersed in the NiMCF-9.2T(R) catalyst, as confirmed by SEM-EDX analysis results.

ACKNOWLEDGEMENT

Research university (RU) grant from Universiti Sains Malaysia to support this research work is gratefully acknowledged. Lilis Hermida also thanks the Directorate General of Higher Education (DIKTI), Ministry of National Education of Indonesia for her PhD scholarship

REFERENCES

[1] F. A. Twaiq, A. R.Mohamed and S. Bhatia. Liquid hydrocarbon fuels from palm oil by catalytic cracking over aluminosilicate mesoporous catalysts with various Si/Al ratios. *Micropor. Mesopor. Mat.* 2003, **64**: 95–107.

[2] A. G. M. Top. Production and utilization of palm fatty acid distillate (PFAD). *Lipid Technology*. 2010, **22** (1) :11-13

[3] S.Lestari ,P. Maki-Arvela, J. Beltramini, G. Q. M. Lu and D. Y. Murzin. Transforming triglycerides and fatty acids into biofuels. *Chem.Sus.Chem*. 2009, **2**:1109 – 1119.

[4] S. Lestari, P. Maki-Arvela, I. Simakova, J. Beltramini, G. Q. Max Lu and D. Y. Murzin. Catalytic deoxygenation of stearic acid and palmitic acid in semibatch mode. *Catal. Lett*. 2009, **130**: 48–51.

[5] M.J. Murphy, J.D. Taylor and R.L. McCormick. Compendium of experimental cetane number data. National Renewable Energy Laboratory, Colorado, 2004, 1–48.

[6] E.W. Ping, R. Wallace, J. Pierson, T.F. Fuller and C. W. Jones. Highly dispersed palladium nanoparticles on ultra-porous silica mesocellular foam for the catalytic decarboxylation of stearic acid. *Micropor. Mesopor. Mat.* 2010, **132**: 174–180.

[7] Y. Han, S.S. Lee and J.Y. Ying. Siliceous mesocellular foam for high-performance liquid chromatography: Effect of morphology and pore structure. *J. Chromatogr. A.* 2010, **1217**:4337–4343.

[8] R.Nares, J. Ramırez, A. Gutierrez-Alejandre and R. Cuevas. Characterization and hydrogenation activity of Ni/Si(Al)-MCM-41 catalysts prepared by deposition-precipitation. *Ind. Eng. Chem. Res.* 2009, **48**: 1154–1162.

[9] P. Schmidt-Winkel, W.W. Lukens,P. Yang, D.L. Margolese, J.S. Lettow, J.Y. Ying and G.D. Stucky. Microemulsion templating of siliceous mesostructured cellular foams with well-defined ultralarge mesopores. *Chem. Mater*. 2000, **12**: 686-696.

[10] P. Schmidt-Winkel, C.J. Glinka and G.D. Stucky. Microemulsion templates for mesoporous silica. *Langmuir*, 2000, **16**:356- 361.

[11] K.S.W. Sing. Adsorption methods for the characterization of porous materials. *Adv. Colloid Interface Sci.*1998, **76 – 77:** 3-1.

[12] T.J. Barton, L.M. Bull, W.G. Klemperer, D.A. Loy, B. McEnaney, M. Misono, P.A. Monson, G. Pez, G.W. Scherer, J.C. Vartuli and O.M. Yaghi. Tailored porous materials. *Chem. Mater.* 1999, **11**: 2633-2656.

[13] K.S.W.Sing, D.H. Everett, R.A.W. Haul, L. Moscou, R.A. Pierotti, J. Rouquerol and T. Siemieniewska. Reporting physisorption data for gas/solid systems with special reference to the determination of surface area and porosity. *Pure Appl. Chem.* 1985, **57**: 603–619.

[14] H.S. Roh, I.H. Eum, D.W. Jeong, B.E. Yi, J.G. Nab and C.H. Ko. The effect of calcination temperature on the performance of $Ni/MgO–Al_2O_3$ catalysts for decarboxylation of oleic acid. *Catal. Today*. 2011, **164**: 457–460.

[15] D.D. Do. Adsorption Science and Technology: Proceeding of the Second Pacific Basin Conference on Adsorption

Science and Technology, World Scientific Publishing Co. Pte. Ltd, Singapore, 2000.